Gradient Polymeric Materials Based on Poorly Compatible Epoxy Oligomers

L. M. Amirova, K. A. Andrianova

Tupolev Kazan State Technical University, 10 Karl Marx Street, 420111 Kazan, Russia

Received 1 December 2004; accepted 20 June 2005
DOI 10.1002/app.23099
Published online in Wiley InterScience (www.interscience.wiley.com).

ABSTRACT: Gradient materials developed on the basis of poorly compatible epoxy oligomers are proposed. The influence of the composition and curing conditions on the stratification of the compounds was studied. The distribution of the components of the curing systems was determined by Fourier transform infrared and elemental analysis. The microhardness and glass-transition temperature varied across the section as a function of the component content and curing temperature. © 2006 Wiley Periodicals, Inc. J Appl Polym Sci 102: 96–103, 2006

Key words: incompatibility; oligomers; phase diagrams

INTRODUCTION

Polymer systems with spatial changes in properties, so-called gradient materials, have attracted increasing interest in recent years.[1] The property gradient in such materials is caused by the variation of the chemical composition, whereas the spatial extension of the gradient may differ.[2] Because of their unique nature, these materials are widely applied as implants in biomedicine and as protective shock-proof coatings and isolation materials in engineering. Optical materials with a gradient refractive index (i.e., GRIN materials) attract special interest.[3–5] Such objects are applied in optoelectronics and fiber optics as light-focusing elements, fibers,[6–8] and sensors.[9]

The investigation of the properties of gradient materials is complex because these systems cannot be completely characterized by known constants of materials. In this connection, special models for the characterization of the behavior of gradient materials have been developed.[10,11] The majority of the information on gradient materials concerns their mechanical and thermal properties,[12–14] including the distribution of the elasticity modulus and the factor of thermal expansion.[15,16] In general, the gradient materials possess enhanced properties in comparison with homopolymers.[17]

The different ways of producing materials with gradients of structure and properties have been the subject of a number of works.[18] Ultrathin gradient polymeric films with a thickness about 1.5 nm were obtained by grafting.[19] Gradient copolymers may be produced also by ionic and radical polymerization.[20]

The methods of obtaining gradient materials based on interpenetrating polymer networks are well known.[21–23] Gradient interpenetrating polymer networks are a special class of polymer blends consisting of two independent networks, of which at least one has been synthesized and/or crosslinked in the presence of the other. Such systems contain a spatial variation or gradient in the concentration of the components across the thickness. Another potential method of obtaining gradient materials is the diffusion of a monomer into an incompletely crosslinked polymeric matrix with subsequent polymerization.[24–26]

In this study, a method of manufacturing gradient polymeric materials from blends of a poorly compatible aromatic epoxy resin and glycidyl esters of phosphorus acid (GEPAs) is suggested. It has been previously shown that GEPAs are potential agents for development binders for composite materials,[27] optical materials,[28] polymeric materials with low flammability,[29] and metal-containing epoxy polymers.[30] During the study, it was found that the limited compatibility of blends of GEPAs with an aromatic epoxy oligomer allowed the prediction of the creation of gradient materials on their basis. The spontaneous stratification of components due to the difference in the densities of phases is the driving force of the gradient of structure in such systems. The degree of stratification depends also on the percentage, viscosity, interfacial tension of blends,[31]

Correspondence to: K. A. Andrianova (tina_a@mail.ru).
Contract grant sponsor: Program Civilian Research and Development Foundation (CRDF) and Russian Federal Ministry of Education and Science (BRHE, REC-007); contract grant number: Y2-E-07-07.

Journal of Applied Polymer Science, Vol. 102, 96–103 (2006)

TABLE I
Characteristics of the Epoxy Compounds

Epoxy compound	Epoxy number (%)	Molecular weight	Density (g/cm^3)
ED-20	21	410	1.1660
TGP	48	266	1.3673

and other factors that can be regulated to produce materials with necessary properties.

EXPERIMENTAL

Materials

The aromatic epoxy resin ED-20 (73% diglycidyl ether of bisphenol A monomer; Ufa Chemical Factory, Russia) and triglycidyl phosphate

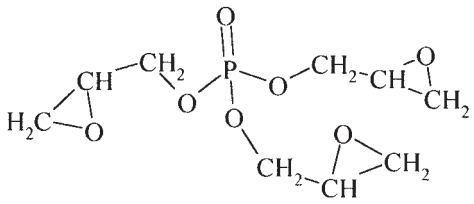

(TGP; synthesized and purified according to ref. 32) were used as the epoxy compounds. Some of their characteristics are presented in Table I. 4,4′-Diamino diphenylmethane (DDM) with a density value of 1.15 g/cm^3 was used as the curing agent.

Study of the compounds

The compatibility of ED-20 with TGP was evaluated microinterferometrically with an MI-2 device (LOMO, St. Petersburg, Russia). The phase diagram was constructed on the basis of obtained data.

For the quantitative description of the systems characterized by a absence of preliminary data on the range of particle sizes and their composition, the turbidity method was applicable.[33] Therefore, the size and size distribution of emulsion particles in the ED-20/TGP system were evaluated from the turbidity spectra.

The viscosity of the epoxy oligomer mixture was measured with a Hoeppler viscosimeter KF3.2 (Rheotest, Germany).

Synthesis

Compositions of ultimate incompatibility containing 30, 35, or 40 mass % TGP were chosen for producing the gradient materials. To obtain emulsions, the components were mixed with an amalgamator (Semico, Novosibirsk, Russia) operating at a speed of 200–500 min^{-1}. The time of mixing was 5–20 min. Films with a thickness up to 100 μm were prepared via pouring on a polytetrafluoroethylene surface. Samples with a thickness of 10 mm were prepared by the filling of block forms.

Characterization

Attenuated total reflection/Fourier transform infrared (ATR–FTIR) spectroscopy was used to characterize the stratification of the components. The IR spectra of the upper and lower surfaces were recorded with a Bruker IFS-66 V/S Fourier transform spectrometer (Ettlingen, Germany) with a KRS-5 prism. The depth of penetration was 2 ± 0.5 mcm.

The quantitative distribution of TGP across the thickness was determined by elemental analysis. For this purpose, samples 10 mm thick were prepared. Cuts in the material of 1-mm thickness from the surface were made with a microtome. Then, in each cut, the content of phosphorus was determined, and the recalculation of the concentration of TGP was carried out.

The thermomechanical curves were registered by the penetration on a section of the sample along a gradient of the concentration, and this permitted the determination of the glass-transition temperature (T_g) distribution. The curves were obtained with a 120 grad/h speed of heating at a static loading of 9.8 N. The diameter of the penetrant cross section was 2 mm. The change in the microhardness across the thickness of the material was determined with a PMT-3 instrument (LOMO, St. Petersburg, Russia) with the size of a diamond needle imprint.

RESULTS AND DISCUSSION

Study of the compounds

The compatibility of the components plays a great role in producing polymers with spontaneous stratifica-

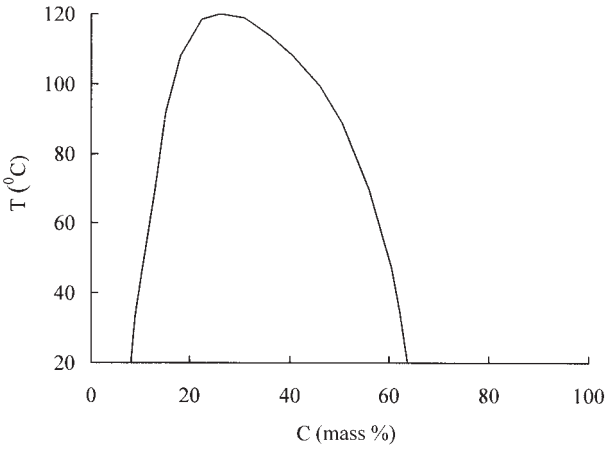

Figure 1 Phase diagram of the ED-20/TGP system (T = temperature, C = TGP concentration).

TABLE II
Properties of the Blends of the Epoxy Compounds

TGP (mass %)	Particle size (nm)	Gel time (min)[a]	Size of zones (mm)		
			h_1	h_2	h_3
30	125 ± 25	100	5	3,1	1,9
35	151 ± 29	80	3	5	2
40	127 ± 23	60	1,5	4,5	4

[a] T_c = 20°C.

h_1, h_2, h_3 are the heights of areas formed across the section of a sample as a result of stratification.

tion. In this work, the compatibility of the epoxy compounds was studied with the microinterferometric method. The phase diagram of the ED-20/TGP system at 20°C is shown on Figure 1. The full compatibility of the components could be observed at TGP concentrations below 8 mass % and over 64 mass %. The components showed incompatibility in the middle range of concentrations, with a solubility upper critical temperature of 120°C.

According to the results of a light-dispersion study, in the incompatibility range, all the compounds formed fairly stable emulsions with particle sizes of

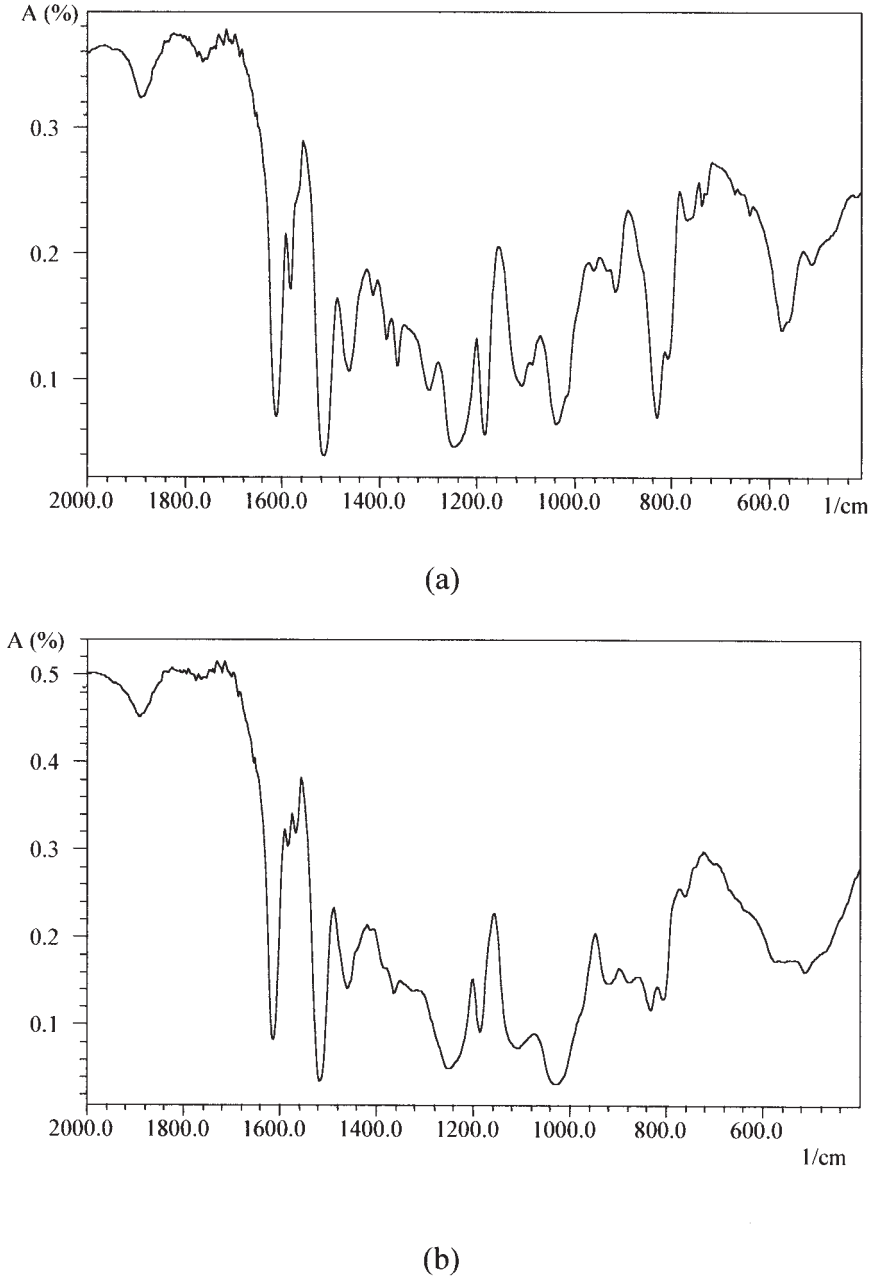

Figure 2 Attenuated total reflection IR spectra of (a) the upper surface and (b) the lower surface of the ED-20/TGP system (TGP concentration = 30 mass %, A = normalized absorption).

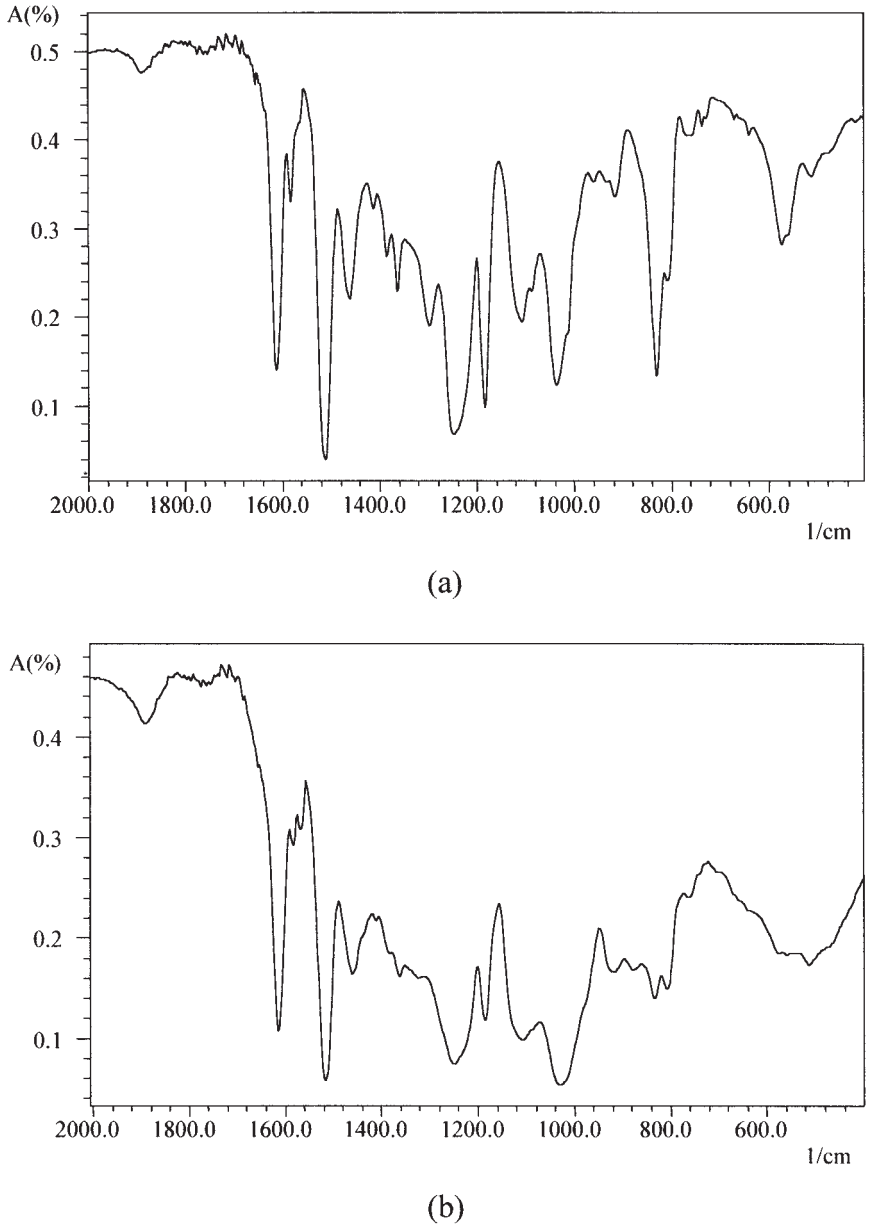

Figure 3 Attenuated total reflection IR spectra of the ED-20/TGP system with (à) 8 and (b) 64 mass % TGP (A = normalized absorption).

100–180 nm. Low interfacial tension is known to be a condition for emulsion formation from two poorly limited liquids. In this case, the emulsification of one component in another was possible because of the action of mechanical forces during mixing. Such an emulsion is a steady system, and for its existence, any emulsificator is required.

At the first moment, the mixture presented the emulsion of one phase with a lower density in another phase with a higher density. The continuous phase was TGP saturated with ED-20 because the viscosity of the ED-20/TGP mixture with an epoxy phosphate concentration greater than 10 mass % was close to the viscosity of a solution of TGP saturated with ED-20. Eventually, the floating-up of emulsion particles began because of the difference in the phase densities. As the density of the phase of ED-20 saturated with TGP was less, stratification occurred as a result of the floating of the particles of the aromatic epoxy oligomer. The rate of floating-up of the emulsion particles with radius r can be described by the Stokes approximation:

$$6\pi r\mu(t)\frac{dy}{dt} = \frac{4\pi}{3}r^3 g(\rho_1 - \rho_2),\ (t) = \mu_0 \exp(t / \tau_g) \tag{1}$$

where ρ_1 and ρ_2 are the densities of heavy and light phases, g is the acceleration of free fall, $y(t)$ is the

coordinate of the center of an emerging particle, $\mu(t)$ is the factor of the dynamic viscosity of the denser phase, and τ_g is the gel time of the system.

On the basis of calculations with the aforementioned equation, we found that three areas were formed across the section of a sample during stratification. The top layer became saturated with particles of the emulsion of TGP in ED-20. These particles were the largest, so over time they coalesced and formed their own phase. Thus, the top layer represented a homogeneous solution of TGP in ED-20. The bottom layer was impoverished of emulsion particles because they floated up and represented a homogeneous solution of ED-20 in TGP. The medium layer represented an emulsion of particles whose average size in due course decreased because of the floating-up of larger particles. The area magnitudes for systems with various contents of TGP are given in Table II. The thickness of the top and bottom zones was calculated on the basis of the Stocks equation. The radii of the particles used in this equation were determined from the size distribution of the particles. The thickness of the medium zone represented the difference between the thickness of the whole sample and the sum of the thicknesses of the top and bottom areas.

The stratification was sharply delayed as the viscosity of the compounds grew over the course of curing. The curing rate depended on the composition and temperature of the medium. The gel time was determined from the viscosity growth curves over the course of the crosslinking of the oligomeric systems. Table II presents the gel times for various compounds and temperatures. An increase in the TGP content, as well as heating, accelerated gelation and froze stratification. As a result of the curing of systems with different compositions at different temperatures, materials with variable gradients of the component concentrations and hence controllable structures and properties were prepared.

Characterization of the gradient materials by ATR–FTIR

The component distribution in the upper and lower layers of the materials was evaluated from ATR–FTIR spectra of the upper and lower surfaces.

The absorption bands of the P—O—C group (1040 cm^{-1}) and P═O group (1270 cm^{-1}) from TGP and those of the benzene ring (830 and 1610 cm^{-1}) from ED-20 were used for analysis. Figure 2 shows fragments of spectra of the upper and lower surfaces in the gradient system. The intensity ratio of the peaks of the P—O—C and P═O groups and benzene ring was larger for the spectra of the lower surface [Fig. 2(b)], whereas on the spectra of the upper layer, these peaks were almost equal [Fig. 2(a)].

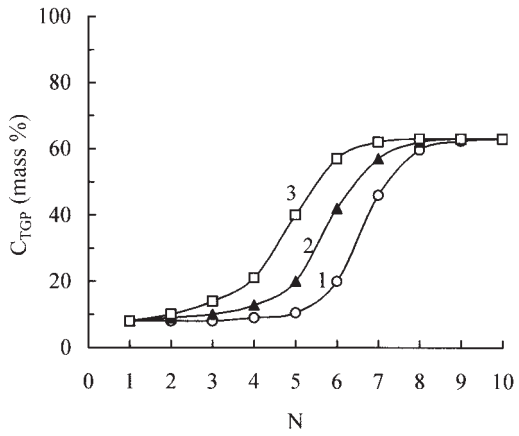

Figure 4 Distribution of TGP in the layers of the ED-20/TGP/DDM system at different concentrations of TGP in the oligomeric blend: (1) 30, (2) 35, and (3) 40 mass % (N = number of layers beginning from the surface, T_c = 20°C). C_{TGP} is the concentration of TGP.

Figure 3 presents ATR–FTIR spectra of compositions with 8 and 64 mass % TGP. As the phase diagram shows, these compositions were compatible, and the concentration of TGP was invariable across the thickness of the material. The spectrum of the mixture with a concentration of 8 mass % TGP [Fig. 3(a)] and the spectrum of the upper layer of the material [Fig. 2(a)] were analogous. Also similar were the spectra of the mixture with 64 mass % TGP [Fig. 3(b)] and the bottom layer of the ED-20/TGP mixed polymer [Fig. 2(b)].

The obtained data indicate that a gradient material was formed with the curing of the stratifying ED-20/TGP blends. Its upper layer consisted of ED-20 containing about 8 mass % TGP, whereas the concentration of TGP at the bottom was about 64 mass %.

Elemental analysis

The distribution of ED-20 and TGP across the section of a gradient sample was determined by elemental analysis. The chemical analysis was sufficient because phosphorus was contained in only one component (TGP). The content of TGP was calculated with the phosphorus content in TGP.

Of particular interest is the analysis of the dependence of the TGP distribution on a section of gradient samples produced from the initial oligomeric blends with different contents of TGP. Figure 4 shows the distribution curves of TGP at various concentrations of TGP: 30, 35, and 40 mass %. The variation of the epoxy phosphate concentration practically did not influence the distribution profile of TGP on a section of the sample but allowed the regulation of the thickness of the layers. The rise of the TGP concentration in the initial system led to an increase in the thickness of the

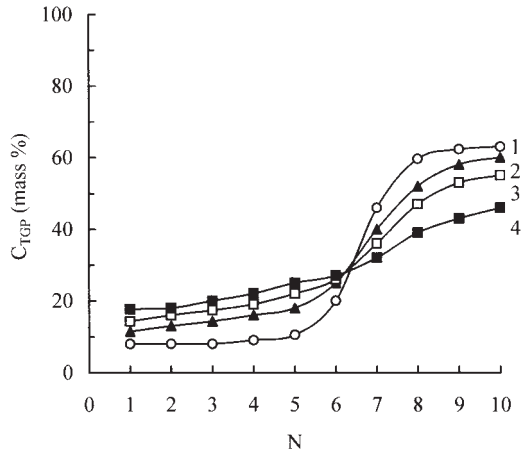

Figure 5 Distribution of TGP in the ED-20/TGP/DDM system at T_c values of (1) 20, (2) 50, (3) 70, and (4) 100°C (concentration of TGP = 30 mass %, N = number of layers beginning from the surface). C_{TGP} is the concentration of TGP.

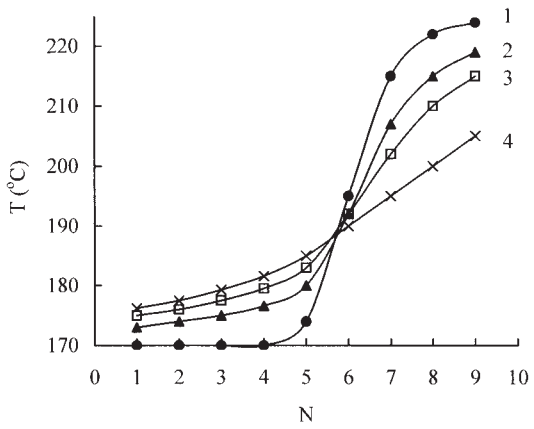

Figure 7 T_g distribution across the thickness of gradient samples of the ED-20/TGP/DDM polymer at T_c values of (1) 20, (2) 50, (3) 70, and (4) 100°C (TGP concentration = 30 mass %, temperature of annealing = 150°C, T = temperature, N = number of layers beginning from the surface).

layer containing 64 mass % TGP. The concentration of TGP in the upper layer was always about 8 mass %, which corresponded to its ultimate solubility in ED-20 at 20°C. In the lower layer, the TGP concentration was 64 mass %. The thickness of the zones obtained from the elemental analysis correlated well with the sizes of the zones calculated with the Stocks equation (Table II).

Figure 5 shows the TGP distribution in the ED-20/TGP/DDM systems obtained at different curing temperatures (T_c's). With increasing T_c, the concentration of TGP in the upper layer increased from 8 (T_c = 20°C) to 18 mass % (T_c = 100°C). In addition, T_c influenced the character of the TGP distribution in the layers of the gradient material. With increasing T_c, the gel time was reduced, and the system was less stratified. As a result, we saw a flatter curve for the TGP distribution (Fig. 5, curve 4).

Thermomechanical analysis and microhardness

Figure 6 illustrates the change in T_g with the height of samples with different concentrations of TGP. The profile of the T_g distribution across the section was similar to the distribution of TGP. Herewith, T_g of the upper layer corresponded to T_g of samples from ED-20 saturated with TGP curing by DDM, whereas T_g of the lower layer corresponded to T_g of cured samples of TGP saturated by ED-20 with 64 mass % TGP.

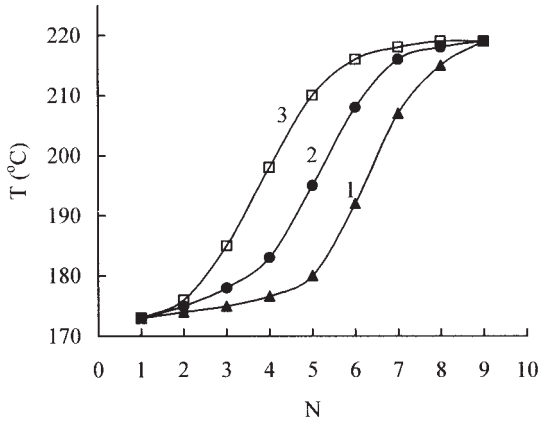

Figure 6 T_g distribution across the thickness of gradient samples of the ED-20/TGP/DDM polymer with TGP concentrations of (1) 30, (2) 35, and (3) 40 mass % (T_c = 50°C, T = temperature, N = number of layers beginning from the surface).

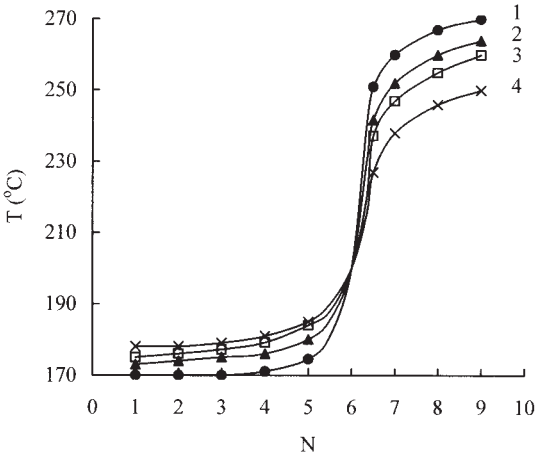

Figure 8 T_g distribution across the thickness of gradient samples of the ED-20/TGP/DDM polymer at T_c values of (1) 20, (2) 50, (3) 70, and (4) 100°C (TGP concentration = 30 mass %, temperature of annealing = 170°C, T = temperature, N = number of layers beginning from the surface).

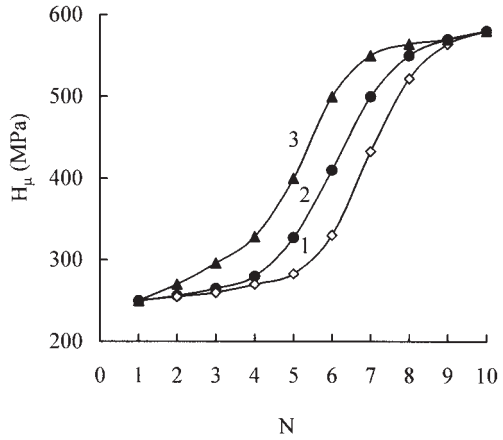

Figure 9 Changes in the microhardness (H_μ) across the thickness of gradient samples of the ED-20/TGP/DDM polymer at TGP concentrations of (1) 30, (2) 35, and (3) 40 mass % (T_c = 50°C, N = number of layers beginning from the surface).

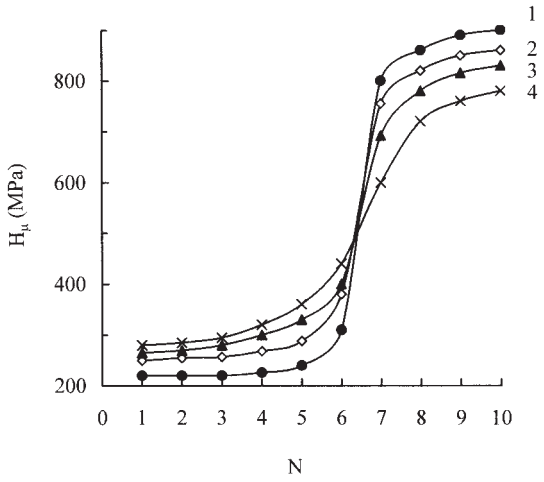

Figure 11 Changes in the microhardness (H_μ) across the thickness of gradient samples of the ED-20/TGP/DDM polymer obtained at T_c values of (1) 20, (2) 50, (3) 70, and (4) 100°C (TGP concentration = 30 mass %, N = number of layers beginning from the surface, temperature of annealing = 170°C).

The T_g distribution across the section of gradient samples at different T_c values is plotted in Figure 7. T_g of the ED-20/TGP/DDM system was in the range of 170–220°C. As T_c increased, T_g varied smoothly, and that fit well with the TGP distribution on a section. The annealing of the sample at 170°C raised T_g of the lower layers up to 270°C (Fig. 8). The last fact may be explained by a gradual increase in the crosslinking density with heating at 170°C, caused by an interaction between hydroxyl and phosphoric groups accompanied by the splitting of water molecules.[34]

The distribution of the microhardness across the section was similar. As one can see in Figure 9, for samples with different concentrations of TGP, the microhardness varied likewise. This correlation was caused by the increase in the crosslink density of the polymer parts enriched by TGP.

Figure 10 illustrates the changes in the microhardness of samples cured at various temperatures. With an increase in T_c, the curve of the change in the microhardness on a section became smooth, and a heat treatment at 170°C raised the microhardness of the lower layers up to 900 MPa (Fig. 11).

The obtained data indicate that the T_g distribution and microhardness across the section of gradient materials could be controlled by changes in the composition within the area of incompatibility, T_c, and heat treatment at 170°C.

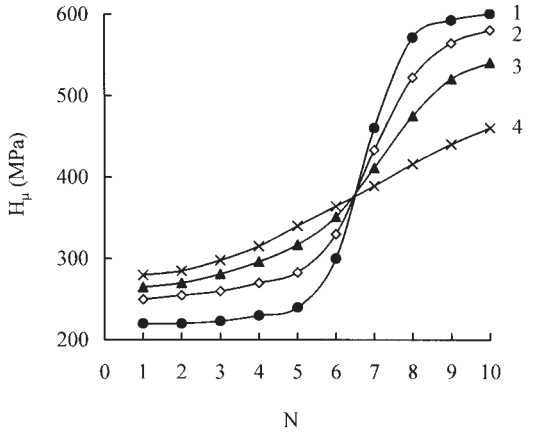

Figure 10 Changes in the microhardness (H_μ) across the thickness of gradient samples of the ED-20/TGP/DDM polymer obtained at T_c values of (1) 20, (2) 50, (3) 70, and (4) 100°C (TGP concentration = 30 mass %, N = number of layers beginning from the surface, temperature of annealing = 150°C).

CONCLUSIONS

Gradient materials based on poorly compatible epoxy compounds were developed. ATR–FTIR spectroscopy and elemental analysis data confirmed that in a certain concentration region, the ED-20/TGP blend was stratified, and a gradient material could be produced by its curing. Its upper layer consisted of ED-20 containing 8 mass % TGP, whereas its lower layer contained up to 64 mass % TGP. T_g and the microhardness increased from the top surface to the bottom part of a sample because of an increase in the crosslinking density in the bottom zone enriched by TGP. These parameters may be regulated by changes in the TGP concentration and T_c and via annealing at 170°C.

References

1. Kryszewski, M. Polym Adv Technol 1998, 9, 244.
2. Neubrand, A. Encyclopedia of Materials: Science and Technology; Elsevier Science Ltd.: Amsterdam, 2001; pp 3407–3413.

3. Ishigure, T.; Hirai, M.; Sato, M.; Koike, Y. J Appl Polym Sci 2004, 91, 404.
4. Ishigure, T.; Hirai, M.; Sato, M.; Koike, Y. J Appl Polym Sci 2004, 91, 410.
5. Masere, J.; Lewis, L. L.; Pojman, J. A. J Appl Polym Sci 2001, 80, 686.
6. Liu, J. H.; Wang, H. Y.; Hsieh, C. D. Macromol Chem Phys 2001, 202, 2980.
7. Liu, J. H.; Chen, J. L.; Wang, H. Y.; Tsai, F. R. Macromol Chem Phys 2000, 201, 126.
8. Liu, J. H.; Chen, J. L.; Wang, H. Y.; Tsai, F. R. Macromol Mater Eng 2000, 274, 31.
9. Zubia, J.; Arrue, J. Opt Fiber Technol 2001, 7, 101.
10. Huang, G. Y.; Wang, Y. S. Eng Fracture Mech 2004, 71, 1841.
11. Jin, Z.-H.; Dodds, R. H., Jr. Eng Fracture Mech 2004, 71, 1651.
12. Guo, L.-C.; Wu, L.-Z.; Zeng, T.; Ma, L. Compos Struct 2004, 64, 433.
13. Tsora, P.; Friedrich, K. Compos A 2003, 34, 75.
14. Krumova, M.; Klingshirn, C.; Haupert, F.; Friedrich, K. Compos Sci Technol 2001, 61, 557.
15. Andrianova, K. A.; Amirova, L. M.; Sidorov, I. N. Book of Abstracts, 12th International Conference on the Mechanics of Composite Materials, Riga, Latvia, 2002; p 11.
16. Andrianova, K. A.; Sidorov, I. N.; Amirova, L. M. Book of Abstracts, 31st Summer School Conference on Advanced Problems in Mechanics, St. Petersburg, Russia, 2003; p 23.
17. Martin, G. C.; Enssani, E.; Shen, M. J Appl Polym Sci 1981, 26, 1465.
18. Kieback, B.; Neubrand, A.; Riedel, H. Mater Sci Eng A 2003, 362, 81.
19. Zdyrko, B.; Klep, V.; Luzinov, I.; Minko, S.; Sydorenko, A.; Ionov, L.; Stamm, M. Polym Prepr 2003, 44, 522.
20. Matyjaszewski, K.; Ziegler, M. J.; Arehart, S. V.; Gresta, D.; Pakula, T. J Appl Phys Org Chem 2000, 13, 775.
21. Elsabee, M. Z.; Dror, M.; Berry, G. C. J Appl Polym Sci 1983, 28, 2151.
22. Mueller, K. F.; Heiber, S. J. J Appl Polym Sci 2003, 27, 4043.
23. Karabanova, L.; Pissis, P.; Kanapitsas, A.; Lutsyk, E. J Appl Polym Sci 1998, 68, 161.
24. Jasso, C. F.; Martinez, J. J.; Mendizabal, E.; Laguna, O. J Appl Polym Sci 2003, 58, 2207.
25. Agari, Y.; Shimada, M.; Ueda, A.; Nagai, S. Macromol Chem Phys 2003, 197, 2017.
26. Akovali, G. J Appl Polym Sci 1999, 73, 1721.
27. Amirova, L. M.; Saifutdinov, R. K.; Magsumova, A. F.; Amirov, R. R. Russ J Appl Chem 2001, 74, 1943.
28. Amirova, L. M.; Stroganov, V. F.; Sakhabieva, E. V. Int J Polym Mater 2000, 47, 43.
29. Amirova, L. M.; Sakhabieva, E. V. Russ J Appl Chem 2001, 74, 1744.
30. Amirova, L. M.; Fomin, V. P.; Amirov, R. R. Russ J Appl Chem 2003, 76, 1835.
31. Xie, X.-M.; Xiao, T.-J.; Zhang, Z.-M.; Tanioka, A. J Colloid Interface Sci 1998, 206, 189.
32. Rizpolozjenskii, N. I.; Zvereva, M. A.; Stepashkina, L. V. Chemistry of Organic Compounds of Phosphorus; Nauka: Leningrad, 1967; p 202.
33. Klenin, V. J. Thermodynamics of Systems Containing Flexible-Chain Polymers; Elsevier: Amsterdam, 1999.
34. Amirova, L. M. Polym Sci 2003, 45, 896.